The Interaction of Water and Dibromine in the Gas Phase: An Investigation of the Complex $H_2O\cdots Br_2$ by Rotational Spectroscopy and Ab Initio Calculations

Anthony C. Legon,*[a] Jennifer M. A. Thumwood,[a] and Eric R. Waclawik[a, b]

Abstract: The ground-state rotational spectra of eight isotopomers of a complex formed by water and dibromine in the gas phase were observed by pulsed-jet, Fourier transform microwave spectroscopy. The spectroscopic constants B_0, C_0, Δ_J, Δ_{JK}, $\chi_{aa}(Br_x)$ (x = i for inner, o for outer), $\{\chi_{bb}(Br_x)-\chi_{cc}(Br_x)\}$ and $M_{bb}(Br_x)$ were determined for $H_2O\cdots{}^{79}Br^{79}Br$, $H_2O\cdots{}^{81}Br^{79}Br$, $H_2O\cdots{}^{79}Br^{81}Br$, $H_2O\cdots{}^{81}Br^{81}Br$, $D_2O\cdots{}^{79}Br^{81}Br$ and $D_2O\cdots{}^{81}Br^{81}Br$. For the isotopomers $HDO\cdots{}^{79}Br^{81}Br$ and $HDO\cdots{}^{81}Br^{81}Br$, only $(B_0+C_0)/2$, Δ_J, the $\chi_{aa}(Br_x)$ and $M_{bb}(Br_x)$ were determinable. The spectroscopic constants were interpreted on the basis of several models of the complex to give information about its geometry, binding strength and the extent of electronic rearrangement on complex formation. The molecule $H_2O\cdots Br_2$ has C_s symmetry with a pyramidal configuration at O. The zero-point effective quantities $r(O\cdots Br_i)=2.8506(1)$ Å and $\phi_0=46.8(1)^\circ$, where ϕ is the angle between the C_2 axis of H_2O and the $O\cdots Br-Br$ internuclear axis, were obtained under the assumption of monomer geometries unchanged by complexation. Ab initio calculations, carried out at the aug-cc-pVDZ/MP2 level of theory, gave the equilibrium values $r_e(O\cdots Br_i)=2.7908$ Å and $\phi_e=45.7^\circ$ and confirmed the collinearity of the $O\cdots Br-Br$ nuclei. The potential energy function $V(\phi)$, also determined ab initio, showed that the wavenumber required for inversion of the configuration at O in the zero-point state is only 9 cm^{-1}. By interpreting the Br nuclear quadrupole coupling constants, the fractions $\delta(O\rightarrow Br_i)=0.004(5)$ and $\delta\ (Br_i\rightarrow Br_o)=0.050(2)$ of an electron were determined to be transferred from O to Br_i and Br_i to Br_o, respectively, when the complex is formed. The complex is relatively weak, as indicated by the small value $k_\sigma=9.8(2)$ N m^{-1} of the intermolecular stretching force constant obtained from Δ_J. A comparison of the properties, similarly determined, of $H_2O\cdots F_2$, $H_2O\cdots Cl_2$, $H_2O\cdots Br_2$, $H_2O\cdots BrCl$, $H_2O\cdots ClF$ and $H_2O\cdots ICl$ is presented.

Keywords: ab initio calculations · dibromine · donor–acceptor systems · rotational spectroscopy · water

Introduction

Herein we report a characterisation of the complex $H_2O\cdots Br_2$ in the gas phase. The rotational spectra of eight isotopomers were observed by means of a pulsed-jet, Fourier-transform microwave spectrometer and the spectroscopic constants determined therefrom were interpreted to give various properties of $H_2O\cdots Br_2$ in isolation, including its geometry, strength of binding and the extents of inter- and intramolecular electron transfer on complex formation. Ab initio calculations were used to confirm the interpretations of experimental results.

There are several reasons for our interest in the interaction of H_2O and Br_2, the first two of which centre on the reaction given in Equation (1).

$$Br_2 + H_2O \longrightarrow HOBr + HBr \quad (1)$$

Bromine water is a familiar chemical reagent. Investigations of saturated solutions of Br_2 in water show that although the equilibrium lies to the left-hand side at 25 °C it is achieved rapidly.[1] It seems likely that an initial complex $H_2O\cdots Br_2$ is involved at some point in the mechanism for this reaction.

A second interest in $H_2O\cdots Br_2$ lies in the role of reaction (1) in atmospheric ozone destruction. The reverse reaction can proceed on the surface of solid ice in the winter darkness of the polar regions and can thereby convert the

[a] Prof. Dr. A. C. Legon, J. M. A. Thumwood, Dr. E. R. Waclawik
School of Chemistry
University of Exeter
Stocker Road, Exeter, EX4 4QD (UK)
Fax: (+44) 1392-263434
E-mail: a.c.legon@exeter.ac.uk

[b] Dr. E. R. Waclawik
Present address:
School of Chemistry, Physics and Earth Sciences
Flinders University of South Australia
GPO Box 2100, Adelaide 500 (Australia)

  0947-6539/02/0804-0940 $ 17.50+.50/0 *Chem. Eur. J.* **2002**, *8*, No. 4

photochemically inactive bromine reservoir compounds HOBr and HBr into Br_2.[2, 3] In the spring, Br_2 then undergoes photolysis to give Br atoms, which are about 50 times more efficient in ozone destruction in the lower stratosphere than Cl atoms. A characterisation of the $H_2O\cdots Br_2$ interaction would contribute background understanding to this process also.

In addition to its atmospheric and chemical relevance outlined, $H_2O\cdots Br_2$ is of interest as a member of an extended series $H_2O\cdots XY$, where XY is a homo- or heteronuclear dihalogen molecule. We have been systematically investigating this series by means of both rotational spectroscopy and ab initio calculations, with the aim of testing a recent hypothesis that there exists[4, 5] a halogen-bond analogue $B\cdots XY$ of the more familiar hydrogen bond $B\cdots HX$. So far, comparisons of the properties of the two series for a range of Lewis bases B have revealed a parallelism that suggests it is appropriate to describe this interaction $B\cdots XY$ as a halogen bond. In the specific series $H_2O\cdots XY$, the examples where XY is F_2,[6, 7] ClF,[7, 8] Cl_2,[9] BrCl[10] and ICl[11] have already been examined by our combined experimental/computational approach. The present results for $H_2O\cdots Br_2$ allow us, in particular, to look for trends in the properties not only in the series $H_2O\cdots F_2$, $H_2O\cdots Cl_2$ and $H_2O\cdots Br_2$ involving a homonuclear dihalogen but also invite a comparison with the corresponding series $H_2O\cdots$ClF, $H_2O\cdots$BrCl and $H_2O\cdots$ICl in which the Lewis acid is a heteronuclear dihalogen. A question of fundamental interest concerns the extent of electron transfer from H_2O to XY when $H_2O\cdots XY$ is formed. How does this vary with atom X and how does it vary when X is held constant and Y is changed? These, and other, questions can be answered as a result of the gas-phase experiments reported here. The only earlier work on $H_2O\cdots Br_2$ of which we are aware is infrared spectroscopy of the species isolated in cryogenic matrices carried out by Engdahl and Nelander.[12]

Results

Spectroscopic constants: The rotational spectra observed when isotopically normal samples of H_2O and Br_2 were used with the fast-mixing nozzle[13] in our pulsed-nozzle, Fourier-transform microwave spectrometer[14] were characteristic of the vibrational ground state of four nearly prolate, asymmetric-top isotopomers $H_2O\cdots{}^{79}Br^{79}Br$, $H_2O\cdots{}^{81}Br^{79}Br$, $H_2O\cdots{}^{79}Br^{81}Br$ and $H_2O\cdots{}^{81}Br^{81}Br$ of essentially equal abundance and each having a very large value of the rotational constant A_0. Thus, each isotopomer exhibits μ_a, R-branch transitions of the general type $(J+1)_{K_{-1}K_1'}\leftarrow J_{K_{-1}K_1''}$ but with transitions having $K_{-1}\geq 2$ absent, no doubt as a result of effective depopulation of $K_{-1}\geq 2$ rotational energy levels during the supersonic expansion. A more detailed discussion of rotational state cooling is given in the next section.

As a consequence of the small difference B_0-C_0 in each isotopomer, compared with $B_0 + C_0$, the transitions $(J+1)_{1,J+1}\leftarrow J_{1,J}$ and $(J+1)_{1,J}\leftarrow J_{1,J-1}$ are separated from the corresponding $(J+1)_{0,J+1}\leftarrow J_{0,J}$ transition by only a few MHz. Moreover, each of these transitions carries a rich nuclear quadrupole hyperfine structure arising from the presence of the two $I=3/2$ bromine nuclei and extending with observable intensity over a few tens of MHz. As a result, the hyperfine components of the $K_{-1}=0$ and 1 transitions of a given J overlap, so complicating the assignment problem. Another layer of complication is added by the fact that the inner Br atom is very close to the centre of mass of the complex. A given set of $(J+1\leftarrow J)$ transitions of the pair of isotopomers $H_2O\cdots{}^{79}Br^{79}Br$ and $H_2O\cdots{}^{81}Br^{79}Br$ are therefore nearly coincident. The same applies to the isotopic pair $H_2O\cdots{}^{79}Br^{81}Br$ and $H_2O\cdots{}^{81}Br^{81}Br$, although the transitions of this pair are well separated from those of the $H_2O\cdots{}^{79}Br^{79}Br$/$H_2O\cdots{}^{81}Br^{79}Br$ pair. The complexity of observed spectra that results from these properties of $H_2O\cdots Br_2$ may be seen by inspection of Table 1, which gives the observed frequencies and their assignments for the isotopomers of the complex based on H_2O.

The observed frequencies of nuclear quadrupole hyperfine components in transitions of the isotopomers $D_2O\cdots{}^{79}Br^{81}Br$, $D_2O\cdots{}^{81}Br^{81}Br$, $HDO\cdots{}^{79}Br^{81}Br$ and $HDO\cdots{}^{81}Br^{81}Br$ are recorded in Table 2. Transitions $(J+1)_{1K_1'}\leftarrow J_{1K_1''}$ were not observed for the HDO-based isotopomers because they were too weak. The absence of such transitions for these isotopomers, but not for those involving H_2O or D_2O, provides evidence about the nature of the geometry of $H_2O\cdots Br_2$ and will be discussed in the next section.

Nuclear quadrupole hyperfine frequencies of the observed transitions for each isotopomer were fitted in an iterative, nonlinear least squares procedure to give ground-state spectroscopic constants. These are recorded in Table 3 for the four isotopomers based on H_2O while the corresponding quantities for the D_2O and HDO isotopomers are given in Table 4.

The fit was conducted using the computer program written and distributed by Pickett.[15] The Hamiltonian employed was of the form shown in Equation (2).

$$H = H_R - \tfrac{1}{6}\boldsymbol{Q}(Br_i):\nabla\boldsymbol{E}(Br_i) - \tfrac{1}{6}\boldsymbol{Q}(Br_o):\nabla\boldsymbol{E}(Br_o) + \boldsymbol{I}_{Br_i}\mathbf{M}(Br_i)\boldsymbol{J} + \boldsymbol{I}_{Br_o}\boldsymbol{M}(Br_o)\boldsymbol{J} \quad (2)$$

In Equation (2), H_R is the Hamiltonian for the semi-rigid asymmetric rotor in the Watson A reduction[16] and the I^r representation. Centrifugal distortion terms involving greater than the fourth power in the angular momentum operators were not necessary for a good fit and of the quartic terms only those multiplying the coefficients Δ_J and Δ_{JK} were determinable from the observed transition set. In the fits, the rotational constant A_0 for each isotopomer was fixed at its value calculated from the final geometry of the complex (see next section) since observed frequencies did not depend significantly on this quantity. For the HDO isotopomers, the absence of $K_{-1}=1$ transitions meant that only $(B + C)/2$ and Δ_J were determinable, as seen in Table 4 which gives the experimental spectroscopic constants determined in the final cycles of the least-squares fits for the D_2O and HDO isotopomers of the water–bromine complex.

The second and third terms of Equation (2) are energy operators associated with the interaction of the electric quadrupole moments $\boldsymbol{Q}$ (Br_i) and $\boldsymbol{Q}$ (Br_o) of the inner (i) and outer (o) bromine nuclei with the electric field gradients

Table 1. Observed and calculated rotational transition frequencies of $H_2O\cdots{}^{79}Br^{79}Br$, $H_2O\cdots{}^{81}Br^{79}Br$, $H_2O\cdots{}^{81}Br^{81}Br$ and $H_2O\cdots{}^{79}Br^{81}Br$.

						$H_2O\cdots{}^{79}Br^{79}Br$		$H_2O\cdots{}^{81}Br^{79}Br$		$H_2O\cdots{}^{81}Br^{81}Br$		$H_2O\cdots{}^{79}Br^{81}Br$	
$J'_{K_{-1}K_1} \leftarrow J''_{K_{-1}K_1}$		F_1'	$F' \leftarrow$	F_1''	F''	ν_{obs} [MHz]	$\Delta\nu^{[a]}$ [kHz]	ν_{obs} [MHz]	$\Delta\nu^{[a]}$ [kHz]	ν_{obs} [MHz]	$\Delta\nu^{[a]}$ [kHz]	ν_{obs} [MHz]	$\Delta\nu^{[a]}$ [kHz]
4_{04}	$\leftarrow 3_{03}$	5/2	4	1/2	3	8601.8453	0.0	8580.0453	−0.9	8494.6120	0.1	8516.6876	5.0
		7/2	3	5/2	2	8596.1742	2.4	–	–	8489.9782	−1.2	8509.0259	1.0
		7/2	4	5/2	3	8636.3180	−0.6	8613.7795	0.8	–	–	8546.3212	1.2
		7/2	5	5/2	4	8598.0959	2.2	8585.4615	0.1	–	–	8514.5317	−1.5
		9/2	3	7/2	2	–	–	–	–	8491.4726	0.3	–	–
		9/2	4	7/2	3	8594.4551	−2.1	8575.4537	−0.8	8488.4347	−0.2	8507.9473	−1.8
		9/2	5	7/2	4	8596.0865	−1.6	8576.9845	−1.0	8489.8635	−1.3	8509.3455	−0.3
		9/2	6	7/2	5	8573.6577	0.9	8556.4074	2.7	8470.9910	−1.7	8489.6990	−1.2
		11/2	4	9/2	3	8599.4822	−1.1	8582.2133	−1.2	8492.6365	1.2	8510.9537	−0.4
		11/2	5	9/2	4	8605.2884	4.4	8578.7914	5.0	8497.6750	0.0	8514.9785	0.8
		11/2	6	9/2	5	8597.3276	−2.1	8578.0587	0.9	8490.7977	−0.3	8509.6803	−0.5
		11/2	7	9/2	6	8585.8130	0.7	8567.4994	−0.8	8481.1215	−2.1	8499.9699	3.0
4_{13}	$\leftarrow 3_{12}$	5/2	4	1/2	3	–	–	8566.3756	3.6	8481.2055	0.9	8500.0168	−0.1
		7/2	4	5/2	3	8645.7152	1.1	8622.8098	−1.4	–	–	–	–
		7/2	5	5/2	4	8604.1493	0.8	8587.3635	−0.3	8497.1968	−1.2	8520.4245	−1.8
		9/2	4	7/2	3	8620.7199	1.4	8599.9125	0.8	8511.1499	−7.1	8532.5497	4.0
		9/2	5	7/2	4	8626.5350	−0.9	8605.2017	1.1	8515.9738	0.9	8537.6806	−4.2
		9/2	6	7/2	5	8594.3985	−0.4	8575.9468	−1.7	8489.2955	−0.9	8509.4424	−1.8
		11/2	4	9/2	3	8584.0920	1.1	8567.1901	3.1	8480.5682	0.6	8498.2638	−0.1
		11/2	5	9/2	4	8607.0705	1.0	8584.8180	−1.6	8499.8270	1.9	8516.8250	−1.2
		11/2	6	9/2	5	8602.6429	2.2	8583.3393	−0.8	8496.0102	2.4	8514.6935	−1.1
		11/2	7	9/2	6	8580.3610	−1.6	8562.9123	−2.2	8477.2597	0.8	8495.2342	1.8
4_{14}	$\leftarrow 3_{13}$	5/2	4	1/2	3	8573.5493	0.0	8555.1473	−2.2	8470.2195	0.0	8489.0126	−1.6
		7/2	4	5/2	3	8634.5717	1.3	–	–	–	–	8544.4080	0.1
		7/2	5	5/2	4	8592.9309	−0.3	8576.2185	1.3	8486.2362	−0.1	8509.4424	−2.3
		9/2	4	7/2	3	8609.3556	−2.7	8588.6025	−0.9	8500.0776	1.8	8521.4140	1.5
		9/2	5	7/2	4	8615.1797	−0.2	8593.9008	−0.9	8504.8928	−2.7	8526.5483	−1.9
		9/2	6	7/2	5	8582.9563	−3.5	8564.5328	−1.0	8478.1482	0.8	8498.2638	−3.7
		11/2	4	9/2	3	8572.6778	−3.0	8555.8343	−3.0	8469.4433	−2.5	8487.0760	−0.8
		11/2	5	9/2	4	8595.6475	1.0	8573.4090	0.4	8488.6917	−0.8	8505.6319	1.9
		11/2	6	9/2	5	8591.2637	−0.3	8572.0560	−0.5	8484.9150	1.2	8503.5152	−0.5
		11/2	7	9/2	6	8568.9533	0.0	8551.5660	1.5	8466.1367	0.4	8484.0556	2.6
5_{05}	$\leftarrow 4_{04}$	7/2	3	5/2	2	10783.7693	0.0	–	–	10644.5906	−3.8	–	–
		7/2	4	5/2	3	10769.8775	0.5	–	–	10632.9654	−2.2	10656.2932	−0.3
		7/2	5	5/2	4	10748.4370	−1.0	10723.1361	3.6	10615.0380	1.3	10641.0239	−0.3
		9/2	3	7/2	2	10744.9350	1.8	10721.1378	−3.1	10612.2977	−1.2	–	–
		9/2	4	7/2	3	10750.4585	2.2	10726.1103	−1.6	10616.7866	1.7	10641.4859	1.6
		9/2	5	7/2	4	10765.2144	−3.8	10739.6130	−0.5	10629.1365	5.5	10655.2858	−2.3
		9/2	6	7/2	5	–	–	10725.9137	0.5	10614.0611	−6.0	10640.7567	0.6
		11/2	4	9/2	3	10747.4396	−2.9	–	–	10614.2052	1.6	10642.6669	4.5
		11/2	5	9/2	4	–	–	10721.1069	1.4	10612.1837	6.9	–	–
		11/2	6	9/2	5	10742.9735	0.3	10719.2376	−2.5	10610.4777	−1.1	10634.8192	0.1
		11/2	7	9/2	6	10730.1475	−0.5	10707.4803	1.0	10599.6992	0.5	10623.8756	−4.5
		13/2	5	11/2	4	–	–	10724.2329	−0.6	10614.0330	1.6	10637.8122	−0.8
		13/2	6	11/2	5	10750.2343	0.0	10723.1764	−0.7	10616.6176	4.0	10639.7434	−1.2
		13/2	7	11/2	6	10746.4587	2.5	10722.3930	−2.6	10613.3403	−2.2	10637.2184	−3.6
		13/2	8	11/2	7	10738.4751	−1.8	10715.0864	1.1	10606.6450	−1.2	10630.7051	2.2
5_{14}	$\leftarrow 4_{13}$	7/2	3	5/2	2	10777.5052	3.0	–	–	10640.3937	0.8	–	–
		7/2	4	5/2	3	10769.9459	−5.1	10729.3115	−0.5	10634.1326	−2.5	10656.5422	0.1
		7/2	5	5/2	4	10744.4955	1.4	10720.5785	−0.9	10612.7122	0.4	–	–
		9/2	3	7/2	2	10752.2377	1.4	10728.3475	−0.8	10619.2835	0.5	10644.9153	1.2
		9/2	4	7/2	3	10764.2613	−2.2	10739.2583	4.4	10629.2333	1.9	10654.6324	2.8
		9/2	5	7/2	4	10777.3515	0.9	10751.2320	−0.4	10640.1768	−1.6	10666.8415	−1.4
		9/2	6	7/2	5	10754.3555	−0.5	10731.5425	−0.7	10620.8832	2.0	10647.8987	−0.7
		11/2	4	9/2	3	–	–	10744.4157	0.7	10620.0504	0.5	10648.6378	−0.3
		11/2	5	9/2	4	10762.0541	−3.3	10737.2238	−4.9	10627.3630	−0.7	10652.8740	−0.6
		11/2	6	9/2	5	10762.2013	−1.9	10737.3650	0.5	10627.4922	0.6	10652.9285	−4.6
		11/2	7	9/2	6	10743.4592	0.6	10720.2617	0.5	10611.8514	1.0	–	–
		13/2	5	11/2	4	10743.8895	−1.5	10721.2373	0.9	10612.1842	−2.6	10635.5757	−0.4
		13/2	6	11/2	5	10755.9212	1.6	10730.2600	0.2	10622.2700	−0.1	10645.1127	2.6
		13/2	7	11/2	6	10753.1923	1.2	10729.0855	−0.7	10619.9267	1.7	10643.7054	3.5
		13/2	8	11/2	7	10739.1445	0.7	10716.2246	1.1	10608.1186	−0.7	10631.7025	1.5

0947-6539/02/0804-0942 $ 17.50+.50/0 *Chem. Eur. J.* **2002**, *8*, No. 4

Table 1. (Continued).

$J'_{K_{-1}K_1} \leftarrow J''_{K_{-1}K_1}$	F_1'	$F' \leftarrow$	F_1''	F''	$H_2O\cdots{}^{79}Br^{79}Br$		$H_2O\cdots{}^{81}Br^{79}Br$		$H_2O\cdots{}^{81}Br^{81}Br$		$H_2O\cdots{}^{79}Br^{81}Br$	
					ν_{obs} [MHz]	$\Delta\nu^{[a]}$ [kHz]	ν_{obs} [MHz]	$\Delta\nu^{[a]}$ [kHz]	ν_{obs} [MHz]	$\Delta\nu^{[a]}$ [kHz]	ν_{obs} [MHz]	$\Delta\nu^{[a]}$ [kHz]
$5_{15} \leftarrow 4_{14}$	7/2	3	5/2	2	10763.4768	−0.1	10737.4602	0.3	10626.6919	1.0	10652.2994	1.6
	7/2	4	5/2	3	10755.7351	−1.3	10715.0488	−2.5	10620.2732	−0.9	10642.6341	−3.6
	7/2	5	5/2	4	–	–	10706.5008	0.6	10598.9230	1.6	10623.4604	0.7
	9/2	3	7/2	2	10738.0719	1.3	10714.2017	0.9	10605.4597	−1.5	–	–
	9/2	4	7/2	3	10750.0898	−0.9	10725.1591	4.3	10615.4066	2.8	10640.7247	−0.7
	9/2	5	7/2	4	10763.2607	1.2	10737.1973	4.7	10626.4219	2.3	10653.0320	2.0
	9/2	6	7/2	5	10740.2767	3.0	10717.5270	−0.8	10607.1317	2.1	10634.0751	2.6
	11/2	4	9/2	3	–	–	10730.5249	−2.4	10606.3430	−2.4	10634.8805	−4.3
	11/2	5	9/2	4	10747.8612	−1.2	10723.0982	0.2	10613.5168	−0.3	10638.9690	5.7
	11/2	6	9/2	5	10747.9956	−0.6	10723.2244	−1.3	10613.6375	2.5	10639.0053	−3.9
	11/2	7	9/2	6	10729.2158	3.9	10706.0494	0.1	10597.9614	2.1	10622.7777	1.0
	13/2	5	11/2	4	10729.6585	−0.1	10707.0735	−0.8	10598.3083	−1.4	10621.6263	−2.9
	13/2	6	11/2	5	10741.6529	1.1	10716.0442	0.0	10608.3596	−3.0	10631.1578	−1.2
	13/2	7	11/2	6	10738.9780	1.0	10714.9761	−0.2	10606.0638	0.8	10629.7499	2.0
	13/2	8	11/2	7	10724.9117	−1.1	10702.0636	1.4	10594.2428	0.5	10617.7577	1.5
$6_{06} \leftarrow 5_{05}$	13/2	8	11/2	7	–	–	–	–	12725.9205	−2.0	–	–
	15/2	9	13/2	8	–	–	–	–	12730.9764	1.0	–	–
$6_{16} \leftarrow 5_{15}$	9/2	3	7/2	2	–	–	–	–	12729.8340	−1.9	–	–
	9/2	6	7/2	5	–	–	–	–	12723.1905	−1.7	–	–
	11/2	4	9/2	3	–	–	–	–	12726.8258	1.4	–	–
	11/2	7	9/2	6	–	–	–	–	12728.0625	1.4	–	–
	13/2	5	11/2	4	–	–	–	–	12727.8773	−2.1	–	–
	13/2	6	11/2	5	–	–	–	–	12731.4125	3.6	–	–
	13/2	7	11/2	6	–	–	–	–	12730.1046	−0.8	–	–
	13/2	8	11/2	7	–	–	–	–	12719.9839	0.1	–	–
	15/2	6	13/2	5	–	–	–	–	12722.7154	−0.8	–	–
	15/2	7	13/2	6	–	–	–	–	12728.5622	1.5	–	–
	15/2	8	13/2	7	–	–	–	–	12727.1733	−0.6	–	–
	15/2	9	13/2	8	–	–	–	–	12719.1029	−3.9	–	–

[a] $\Delta\nu = \nu_{obs} - \nu_{calcd.}$

Table 2. Observed and calculated rotational transition frequencies of $D_2O\cdots{}^{79}Br^{81}Br$, $D_2O\cdots{}^{81}Br^{81}Br$, $HDO\cdots{}^{79}Br^{81}Br$ and $HDO\cdots{}^{81}Br^{81}Br$.

$J'_{K_{-1}K_1} \leftarrow J''_{K_{-1}K_1}$	F_1'	$F' \leftarrow$	F_1''	F''	$D_2O\cdots{}^{79}Br^{81}Br$		$D_2O\cdots{}^{81}Br^{81}Br$		$HDO\cdots{}^{79}Br^{81}Br$		$HDO\cdots{}^{81}Br^{81}Br$	
					ν_{obs} [MHz]	$\Delta\nu^{[a]}$ [kHz]	ν_{obs} [MHz]	$\Delta\nu^{[a]}$ [kHz]	ν_{obs} [MHz]	$\Delta\nu^{[a]}$ [kHz]	ν_{obs} [MHz]	$\Delta\nu^{[a]}$ [kHz]
$4_{04} \leftarrow 3_{03}$	5/2	4	3/2	3	–	–	–	–	8232.3882	1.8	8212.7201	3.5
	7/2	3	5/2	2	–	–	–	–	8224.6994	−0.9	8208.0507	−1.6
	7/2	4	5/2	3	–	–	–	–	8261.9822	1.4	8241.5786	6.0
	7/2	5	5/2	4	–	–	–	–	8230.2357	−0.1	8209.5856	−5.8
	9/2	3	7/2	2	–	–	–	–	–	–	8209.5846	−2.8
	9/2	4	7/2	3	–	–	–	–	8223.6523	1.4	–	–
	9/2	5	7/2	4	–	–	–	–	8225.0312	−1.0	8207.9492	1.9
	9/2	6	7/2	5	–	–	–	–	8205.4300	−1.0	8189.1087	−2.4
	11/2	4	9/2	3	–	–	–	–	8226.6518	0.8	8210.7241	5.0
	11/2	5	9/2	4	–	–	–	–	8230.6296	−0.5	8215.7072	−3.8
	11/2	6	9/2	5	–	–	–	–	8225.3856	−0.6	8208.8953	−1.3
	11/2	7	9/2	6	–	–	–	–	8215.6928	−1.4	8199.2403	1.3
$5_{05} \leftarrow 4_{04}$	7/2	3	5/2	2	–	–	–	–	–	–	10292.1956	2.4
	7/2	4	5/2	3	–	–	–	–	–	–	10280.5579	2.1
	7/2	5	5/2	4	9957.5629	−0.9	9937.1767	1.0	10285.6475	0.4	10262.6612	−4.3
	9/2	3	7/2	2	–	–	–	–	–	–	10259.8863	−3.1
	9/2	4	7/2	3	9957.9951	2.8	9938.8901	−0.8	10286.0880	−1.1	10264.3890	−3.9
	9/2	5	7/2	4	9971.7810	2.2	9951.2228	−2.9	10299.8775	−6.8	10276.7298	−2.5
	9/2	5	9/2	5	–	–	–	–	–	–	10195.9868	−2.1
	9/2	6	7/2	5	9957.2895	1.6	9936.2171	−2.0	10285.3791	2.8	–	–
	9/2	6	11/2	6	–	–	–	–	–	–	10265.5579	4.8
	11/2	4	9/2	3	–	–	9936.3641	−0.4	10287.2924	−0.9	–	–
	11/2	5	9/2	4	9953.2848	−1.2	–	–	10281.3704	2.3	–	–
	11/2	6	9/2	5	9951.3549	0.6	9932.6080	−1.2	10279.4416	1.1	10258.1019	1.9
	11/2	7	9/2	6	9940.4605	1.1	9921.8644	1.0	10268.5244	−1.9	10247.3387	−0.9
	11/2	7	11/2	7	–	–	–	–	–	–	10460.0194	−2.4
	13/2	5	11/2	4	9954.3516	−0.3	9936.1595	0.6	10282.4358	1.0	10261.6518	4.4
	13/2	6	11/2	5	9956.2523	0.9	9938.6961	−0.6	10284.3516	1.3	10264.2080	4.7
	13/2	7	11/2	6	9953.7690	0.6	9935.4854	0.7	10281.8503	1.6	10260.9689	0.9
	13/2	8	11/2	7	9947.2752	0.7	9928.8070	0.0	10275.3448	0.2	10254.2811	−2.0

Table 2. (Continued).

$J'_{K_{-1}K_1} \leftarrow J''_{K_{-1}K_1}$	F_1'	$F' \leftarrow F_1''$		F''	$D_2O\cdots{}^{79}Br^{81}Br$ ν_{obs} [MHz]	$\Delta\nu$[a] [kHz]	$D_2O\cdots{}^{81}Br^{81}Br$ ν_{obs} [MHz]	$\Delta\nu$[a] [kHz]
$5_{14} \leftarrow 4_{13}$	7/2	5	5/2	4	9958.3165	−0.8	9939.3243	3.2
	9/2	6	7/2	5	9968.9518	2.1	9947.5258	−0.2
	11/2	5	9/2	4	9973.9012	3.5	9953.9652	−3.0
	11/2	6	9/2	5	9973.9508	−1.8	9954.0939	1.0
	11/2	7	9/2	6	9957.7409	−0.9	9938.4590	2.0
	13/2	5	11/2	4	9956.6158	0.5	9938.7958	−0.7
	13/2	6	11/2	5	9966.1230	0.3	9948.8460	−0.2
	13/2	7	11/2	6	9964.7358	1.2	9946.5420	2.0
	13/2	8	11/2	7	9952.7807	−1.0	9934.7707	−0.1
$5_{15} \leftarrow 4_{14}$	7/2	5	5/2	4	9935.7300	−5.4	9916.8168	0.6
	9/2	5	7/2	4	–	–	9944.2843	−0.2
	9/2	6	7/2	5	9946.3785	−0.7	9925.0612	0.6
	11/2	5	9/2	4	–	–	9931.4048	−2.6
	11/2	6	9/2	5	9951.2880	−0.6	9931.5237	0.6
	11/2	7	9/2	6	9935.0657	−1.7	9915.8561	1.1
	13/2	5	11/2	4	9933.9292	1.0	9916.2029	−1.3
	13/2	6	11/2	5	9943.4292	−2.9	9926.2247	1.6
	13/2	7	11/2	6	9942.0418	−0.3	9923.9653	0.6
	13/2	8	11/2	7	9930.0969	−0.8	9912.1816	−0.2
$6_{06} \leftarrow 5_{05}$	9/2	3	7/2	2	11956.0050	−2.5	11932.1305	1.2
	9/2	4	7/2	3	11966.2374	−0.5	11942.2403	0.4
	9/2	5	7/2	4	11953.8522	−3.7	11931.8544	0.5
	9/2	6	7/2	5	–	–	11923.4004	0.5
	11/2	4	9/2	3	11945.5776	−3.4	11921.8635	−0.5
	11/2	5	9/2	4	11949.7182	−0.4	11926.5572	0.4
	11/2	6	9/2	5	11955.0058	0.2	11931.2723	0.2
	11/2	7	9/2	6	11947.2627	0.4	11923.1261	0.9
	13/2	5	11/2	4	11948.3846	0.1		
	13/2	6	11/2	5	11944.6311	6.2	11921.7859	0.4
	13/2	7	11/2	6	–	–	11919.4884	0.1
	13/2	8	11/2	7	11935.2202	1.3	11912.5096	0.6
	15/2	6	13/2	5	11945.0423	−0.1	11922.7461	−1.1
	15/2	7	13/2	6	11946.1381	0.8	11924.1869	−0.6
	15/2	8	13/2	7	11944.5958	−6.0	11922.4420	−1.0
	15/2	9	13/2	8	11940.0087	0.8	11917.5591	2.0
$6_{15} \leftarrow 5_{14}$	9/2	4	7/2	3	11974.1825	2.9	11950.6923	1.
	9/2	5	7/2	4	11964.6702	−3.4	11943.2053	−0.2
	9/2	6	7/2	5	11954.7554	2.2		
	11/2	4	9/2	3	11959.1674	0.7		
	11/2	5	9/2	4	11966.8618	−2.2	11943.2610	−2.2
	11/2	6	9/2	5	11972.0162	−1.4	11947.8852	3.6
	11/2	7	9/2	6	11961.0206	0.2	11936.5536	−8.7
	13/2	5	11/2	4	11961.6520	−1.9	11936.3205	3.7
	13/2	6	11/2	5	11963.3674	0.1		
	13/2	7	11/2	6	11961.9049	−1.2	11938.6627	0.7
	13/2	8	11/2	7	11951.6822	−0.3	11928.5664	−3.4
	15/2	6	13/2	5	11953.3581	0.3		
	15/2	7	13/2	6	11958.8876	2.9	11937.1327	−3.4
	15/2	8	13/2	7	11957.8679	0.8	11935.7455	3.0
	15/2	9	13/2	8	11949.8974	−2.2	11927.7071	2.0
$6_{16} \leftarrow 5_{15}$	9/2	3	7/2	2	11934.3778	7.4		
	9/2	4	7/2	3	–	–	11923.7020	2.4
	9/2	5	7/2	4	11937.5094	1.4	11916.0777	−2.2
	9/2	6	7/2	5	11927.6189	0.3	11904.6721	0.1
	11/2	4	9/2	3	11932.0439	0.1		
	11/2	5	9/2	4	–	–	11916.2155	1.4
	11/2	6	9/2	5	11944.8907	−0.3	11920.8575	0.4
	11/2	7	9/2	6	11933.8940	2.3	11909.5598	−0.2
	13/2	5	11/2	4	11934.5370	−2.2	11909.3610	−0.7
	13/2	6	11/2	5	11936.1829	−4.4	11912.8857	1.2
	13/2	7	11/2	6	11934.7146	1.6	11911.5812	1.1
	13/2	8	11/2	7	11924.4937	1.4	11901.4700	−2.5
	15/2	6	13/2	5	11926.1500	−3.5	11904.1916	−2.1
	15/2	7	13/2	6	11931.6823	2.4	11910.0169	−0.1
	15/2	8	13/2	7	11930.6490	−1.7	11908.6563	0.0
	15/2	9	13/2	8	11922.7008	4.8	11900.6139	0.7

[a] $\Delta\nu = \nu_{obs} - \nu_{calcd.}$

$\nabla\, \boldsymbol{E}$ (Br_i) and $\nabla\, \boldsymbol{E}$ (Br_o) at the respective nuclei, in the usual way. Likewise, the two remaining terms describe the corresponding magnetic coupling of the nuclear spin vectors $\boldsymbol{I}_{Br_i}$ and $\boldsymbol{I}_{Br_o}$ to the rotational angular momentum vector $\boldsymbol{J}$, where $\boldsymbol{M}$ (Br_i) and $\boldsymbol{M}$ (Br_o) are the nuclear spin-rotation coupling tensors.

The matrix of the Hamiltonian H defined in Equation (2) was constructed in the coupled symmetric-rotor basis $\boldsymbol{I}_{Br_i} + \boldsymbol{J} = \boldsymbol{F}_1$, $\boldsymbol{F}_1 + \boldsymbol{I}_{Br_o} = \boldsymbol{F}$ and each F block diagonalised independently. For the H_2O- and D_2O-based isotopomers of the complex, only the diagonal elements $\chi_{aa}(Br_x)$ and $\{\chi_{bb}(Br_x) - \chi_{cc}(Br_x)\}$ (x = i or o) of the nuclear quadrupole coupling tensor $\chi_{\alpha\beta}(Br_x) = -(eQ/h)V_{\alpha\beta}$, where $V_{\alpha\beta} = -\partial^2 V/\partial\alpha\partial\beta$ and $\alpha, \beta = a, b$ or c, were necessary to give fits with a standard deviation σ (see Tables 3 and 4) of a magnitude similar to, or smaller than, the estimated accuracy of frequency measurement (ca. 2 kHz). The off-diagonal elements were therefore assumed to be zero. Similarly, only the diagonal elements M_{bb} (Br_x) and M_{cc} (Br_x) of the Br spin-rotation coupling tensors contributed significantly to the observed frequencies. However, these small quantities were not independently determinable and, in view of the smallness of $\{\chi_{bb}(Br_x) - \chi_{cc}(Br_x)\}$ (see Tables 3 and 4) and of the fact that M_{bb} (Br_x) and M_{cc} (Br_x) are very small, we set M_{bb} (Br_x) equal to M_{cc} (Br_x). For HDO-based isotopomers, only the components χ_{aa} (Br_x) of the Br nuclear quadrupole coupling tensor were determinable from the $K_{-1} = 0$ transitions observed.

Geometry of $H_2O\cdots Br_2$: All observations concerned with the ground-state rotational spectra of the eight isotopomers are consistent with an equilibrium geometry for the complex of the general type shown in Figure 1, that is one of C_s symmetry in which the nuclei of O, Br_i and Br_o lie in the plane of symmetry, with the angle $\phi > 0°$, or one of C_{2V} symmetry ($\phi = 0°$). In either case, the two H atoms are equidistant from a symmetry plane and necessarily the rotational constant $\frac{1}{2}(B_0 + C_0)$ of $HDO\cdots Br_2$ will lie very close to the mean value of this constant for the corresponding $H_2O\cdots Br_2$ and $D_2O\cdots Br_2$ isotopomers. This is found to be so experimentally. For example, the mean value of $\frac{1}{2}(B_0 + C_0)$ for $H_2O\cdots{}^{81}Br^{79}Br$ and $D_2O\cdots{}^{81}Br^{79}Br$ is 1029.636 MHz, while $\frac{1}{2}(B_0 + C_0) =$ 1028.272 MHz for $HDO\cdots{}^{81}Br^{79}Br$. It is

0947-6539/02/0804-0944 $ 17.50+.50/0 Chem. Eur. J. 2002, 8, No. 4

Table 3. Ground-state spectroscopic constants of four isotopomers of $H_2O\cdots Br_2$.

Spectroscopic constant	Isotopomer			
	$H_2O\cdots{}^{79}Br^{79}Br$	$H_2O\cdots{}^{81}Br^{79}Br$	$H_2O\cdots{}^{81}Br^{81}Br$	$H_2O\cdots{}^{79}Br^{81}Br$
B [MHz]	1076.0652(2)	1073.6556(2)	1062.7243(1)	1065.2002(2)
C [MHz]	1073.2268(2)	1070.8300(2)	1059.9556(1)	1062.4187(2)
Δ_J [kHz]	0.298(3)	0.289(3)	0.288(2)	0.295(3)
Δ_{JK} [kHz]	30.02(6)	30.26(6)	29.54(5)	29.42(6)
$\chi_{aa}(Br_i)$ [MHz]	833.331(25)	696.225(18)	696.232(26)	833.391(27)
$\chi_{aa}(Br_o)$ [MHz]	761.811(18)	761.826(25)	636.436(17)	636.412(18)
$\{\chi_{bb}(Br_i)-\chi_{cc}(Br_i)\}$ [MHz]	6.800(50)	5.626(37)	5.740(52)	6.712(60)
$\{\chi_{bb}(Br_o)-\chi_{cc}(Br_o)\}$ [MHz]	0.922(35)	0.924(53)	0.836(37)	0.748(32)
$M_{bb}(Br_i)=M_{cc}(Br_i)$ [kHz][a]	2.6(4)	3.2(3)	3.4(3)	3.0(4)
$M_{bb}(Br_o)=M_{cc}(Br_o)$ [kHz][a]	2.6(4)	2.9(4)	2.7(3)	2.5(4)
N[b]	69	70	87	68
σ [kHz][c]	1.8	1.9	2.1	2.3

[a] Assumed equality, as suggested by the small values of $\{\chi_{bb}(Br)-\chi_{cc}(Br)\}$. [b] Number of transitions in fit. [c] Standard deviation of fit.

Table 4. .Ground-state spectroscopic constants of four deuterium containing isotopomers of $H_2O\cdots Br_2$.

Spectroscopic constant	Isotopomer			
	$D_2O\cdots{}^{79}Br^{81}Br$	$D_2O\cdots{}^{81}Br^{81}Br$	$HDO\cdots{}^{79}Br^{81}Br$	$HDO\cdots{}^{81}Br^{81}Br$
B [MHz]	997.7275(2)	995.8085(2)	–	–
C [MHz]	993.1981(2)	991.2972(2)	–	–
$(B+C)/2$ [MHz]	–	–	1028.2720(3)	1026.1006
Δ_J [kHz]	0.281(2)	0.276(2)	0.299(6)	0.255(6)
Δ_{JK} [kHz]	17.43(5)	17.72(5)	–	–
$\chi_{aa}(Br_i)$ [MHz]	833.428(53)	696.339(42)	833.391(57)	696.391(18)
$\chi_{aa}(Br_o)$ [MHz]	635.529(30)	635.565(30)	635.851(37)	635.761(19)
$\{\chi_{bb}(Br_i)-\chi_{cc}(Br_i)\}$ [MHz]	6.509(37)	5.589(76)	–	–
$\{\chi_{bb}(Br_o)-\chi_{cc}(Br_o)\}$ [MHz]	0.704(66)	0.656(56)	–	–
$M_{bb}(Br_i)=M_{cc}(Br_i)$ [kHz][a]	2.0(4)	3.0(4)	3.4(8)	3.0(4)
$M_{bb}(Br_o)=M_{cc}(Br_o)$ [kHz][a]	2.0(3)	2.1(3)	2.8(6)	2.7(5)
N[b]	71	70	23	26
σ [kHz][c]	2.3	1.9	1.9	3.3

[a] Assumed equality, as suggested by the small values of $\{\chi_{bb}(Br)-\chi_{cc}(Br)\}$. [b] Number of transitions in fit. [c] Standard deviation of fit.

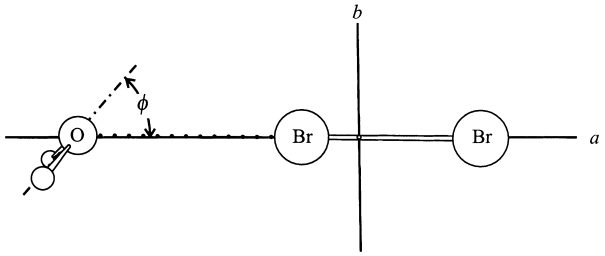

Figure 1. The geometry of the complex $H_2O\cdots Br_2$, drawn to scale, in its principal inertia axis system. The *ab* principal inertia plane is a plane of symmetry. The angle ϕ is the angle between the $O\cdots Br_i$ internuclear axis and the C_2 axis of H_2O. Zero-point values of ϕ and $r(O\cdots Br_i)$ are given in the text.

shown below that the changes in the rotational constants B_0 and C_0 on isotopic substitution at H, Br_i and Br_o lead to a zero-point value $\phi_0=46.8(1)^\circ$, a result in agreement with that from ab initio calculations (see the next section), which confirm that the complex is pyramidal at equilibrium.

Given these conclusions, it remains to establish whether the potential energy barrier to inversion of the configuration at O in the zero-point state ($\phi_0 \rightarrow -\phi_0$) is low enough that the vibrational wavefunctions have C_{2V} symmetry, even though the equilibrium geometry is of C_s symmetry. If this is the case, the complex is referred to as *effectively planar*. In fact, there is evidence from nuclear spin statistical weight effects in the observed spectra of the various isotopomers of $H_2O\cdots Br_2$ which demonstrates conclusively that the complex is either planar at equilibrium or effectively planar in the sense defined.

An effectively planar ($\phi_e>0$, low barrier) or planar ($\phi_e=0$) geometry of the type shown in Figure 1 has the consequence that the operation C_2^a (a two-fold rotation about the *a* axis of the complex) exchanges a pair of equivalent protons in $H_2O\cdots Br_2$ isotopomers and a pair of equivalent deuterons in $D_2O\cdots Br_2$ isotopomers. In the former case, the total wavefunction must be antisymmetric with respect to the operation because protons are $I=\frac{1}{2}$ Fermions, while in the latter case the wavefunction must be symmetric for exchange of equivalent $I=1$ Bosons. The usual arguments for the vibrational ground state of a close shell molecule lead to the conclusion that in $H_2O\cdots Br_2$ rotational energy levels having $K_{-1}=1$ are associated with a nuclear spin statistical weight of 3 relative to a weight of 1 for $K_{-1}=0$ levels. For $D_2O\cdots Br_2$, the ratio is 2:1 for $K_{-1}=0$ relative to $K_{-1}=1$ levels.

Experimental observations confirm qualitatively that such nuclear spin statistical weight effects are indeed present. The transitions $(J+1)_{1,J+1}\leftarrow J_{1,J}$ and $(J+1)_{1,J}\leftarrow J_{1,J-1}$ were certainly more intense than the associated $(J+1)_{0,J+1}\leftarrow J_{0,J}$ transition, although a quantitative measurement of the intensity ratio with a pulsed-jet, Fourier transform microwave spectrometer is unreliable. Given that the $K_{-1}=1$ transitions

have a smaller line strength than the $K_{-1}=0$ transition of the same J and that a depletion of population of $K_{-1}=1$ levels should accompany the supersonic expansion because they are higher in wavenumber by $ch(A-B)\approx 30\ \mathrm{cm}^{-1}$ than $K_{-1}=0$ levels, this observation confirms the presence of the nuclear spin statistical weight effect. On the other hand, the $K_{-1}=1$ transitions of $D_2O\cdots Br_2$ are weaker than the corresponding $K_{-1}=0$ transition, a result consistent with the required 1:2 nuclear spin statistical weight ratio.

It is clear from the foregoing that cooling of $K_{-1}=1$ states during supersonic expansion of the $H_2O/Br_2/Ar$ gas mixture is ineffective and that they retain essentially their room temperature population, even though the expected temperature of the expansion is ≈ 1 K. This result can be readily understood if transfer of population between triplet and singlet nuclear spin states of H_2O is forbidden by a collisional propensity rule.[17] No such rule forbids collisional transfer between $K_{-1}=2$ and $K_{-1}=0$ states, so the former achieve a very low effective temperature and transitions involving $K_{-1}=2$ levels are too weak to observe. In $HDO\cdots Br_2$ isotopomers, the nuclear spin statistical weight effects are absent and hence collisional transfer of population from $K_{-1}=1$ to $K_{-1}=0$ levels is not forbidden. This is why $K_{-1}=1$ transitions were not observed for $HDO\cdots Br_2$.

A high potential energy barrier to the planar conformation of $H_2O\cdots Br_2$ can now be ruled out. In the limit of high barrier, the $v=0$ and $v=1$ levels (which have opposite parity) become degenerate. Nuclear spin statistical weight differences between $K_{-1}=0$ and $K_{-1}=1$ rotational energy levels then disappear. Moreover, collisional transfer of population between $K_{-1}=1$ and $K_{-1}=0$ levels would not be forbidden and $K_{-1}=1$ transitions would be too weak to detect. Both of these consequences of a high barrier are contrary to observation.

The ground-state effective moments of inertia I_b^0 and I_c^0 of the isotopomers $H_2O\cdots{}^{79}Br^{79}Br$, $H_2O\cdots{}^{81}Br^{79}Br$, $H_2O\cdots{}^{79}Br^{81}Br$, $H_2O\cdots{}^{81}Br^{81}Br$, $D_2O\cdots{}^{79}Br^{81}Br$ and $D_2O\cdots{}^{81}Br^{81}Br$ were then fitted to give quantitative details of the geometry shown in Figure 1, the qualitative form of which was established above. The ab initio calculations described in the next section show that the geometries of H_2O and Br_2 change only slightly on complex formation and that the $O\cdots Br_i{-}Br_o$ nuclei deviate insignificantly from collinearity. Accordingly, in the least-squares fit of the experimental moments of inertia, the monomer geometries[18–20] were assumed unchanged from the r_0 values given in Table 5 and a collinear $O\cdots Br_i{-}Br_o$ arrangement was assumed. Then the two parameters that completely define the geometry were determined to be $r(O\cdots Br_i)=2.8496(19)$ Å and $\phi=45.9(17)^\circ$.

It has been demonstrated elsewhere[21] that a better determination of geometry is possible in such cases by a least-squares fit of $(\hbar/\pi)\ (B_0+C_0)\approx I_b^0+I_c^0$. The results obtained by fitting the same group of isotopomers are $r(O\cdots Br_i)=2.8506(1)$ Å and $\phi=46.8(1)^\circ$. They are indeed more precise but agree within experimental error with those from fits of I_b^0 and I_c^0.

Ab initio calculations on $H_2O\cdots Br_2$: The geometry determined in the preceding section is a zero-point quantity because it was obtained by fitting ground-state moments of inertia. It has been shown elsewhere[21] that the angle ϕ_0 that results from fitting I_b^0 and I_c^0 in such complexes is an effective value defined by $\phi_0\approx\cos^{-1}\langle\cos^2\phi\rangle^{1/2}_{0,0}$. The aim of the present section is to obtain an equilibrium value ϕ_e of the angle using ab initio calculations and to determine how the potential energy of $H_2O\cdots Br_2$ varies with ϕ. We shall then use this potential energy function to find a value of $\langle\cos\phi\rangle$ and show that $\cos^{-1}\langle\cos\phi\rangle$ is close to ϕ_0 evaluated from the principal moments of inertia.

Ab initio calculations for $H_2O\cdots Br_2$ were carried out with the GAMESS package[22] and employed the aug-cc-pVDZ basis set.[23, 24] Electron correlation was taken into account at the MP2 level of perturbation theory.[25] Full optimizations were carried out for angles in the range $\phi=0$ to $\pm 90^\circ$, but the geometry was always constrained to have C_s symmetry and the order of the atoms shown in Figure 1. Energies at each point were corrected for basis set superposition error by applying the Boys–Bernardi counterpoise correction procedure.[26] The resulting energies are shown in Figure 2 as a function of the angle ϕ. The full equilibrium ab initio geometry of $H_2O\cdots Br_2$, under the constraint of C_s symmetry and atoms in the order $H_2O\cdots Br{-}Br$, is given in Table 6, where it is compared with the experimental, zero-point version obtained in the preceding section. We note that, given the comparison is of quantities of slightly different definitions, the values $\phi_e=45.8^\circ$ and $r_e(O\cdots Br_i)=2.7908$ Å are in satisfactory agreement with the zero-point quantities $\phi_0=46.8(1)^\circ$ and $r(O\cdots Br_i)=2.8506(1)$ Å. An earlier

Table 5. Properties of some isotopomers of the monomers H_2O and Br_2.

	B_0 [MHz]	C_0 [MHz]	$\chi(^{79}\mathrm{Br})$ [MHz]	$\chi(^{81}\mathrm{Br})$ [MHz]	r_0 [Å]	Angle α [°]
H_2O[a]	435357.7	276138.7	–	–	0.9650[b]	104.8[b]
HDO[a]	272912.6	192055.3	–	–	–	–
D_2O[c]	218038.2	145258.0	–	–	–	–
$^{79}Br_2$	2456.7[d]	2456.7[d]	810.0(5)[e]	-	2.28326[f]	–
$^{79}Br^{81}Br$	2426.4[g]	2426.4[g]	810.0(5)	676.7(4)[h]	–	–
$^{81}Br_2$	2396.1[g]	2396.1[g]	–	676.7(4)	–	–
^{79}Br atom	–	–	769.76[i]	–	–	–
^{81}Br atom	–	–	–	643.03[i]	–	–

[a] Ref. [18]. [b] The r_0 geometry of H_2O/D_2O is the mean of three determined in ref. [18] by using the three possible combinations of principal moments of inertia (I_a, I_b), (I_a, I_c) and (I_b, I_c). [c] Ref. [19]. [d] Ref. [20]. [e] Ref. [35]. [f] Calculated from B_0 for $^{79}Br_2$ using $r_0=(h/8\pi^2\mu B_0)^{1/2}$. [g] Calculated from $B_0=\{h/8\pi^2\mu r_0^2\}$ by using r_0 for $^{79}Br_2$. [h] Calculated from the $^{79}Br_2$ value by using the ratio $^{81}Q/^{79}Q$ of the Br nuclear electric quadrupole moments. [i] Ref. [36].

0947-6539/02/0804-0946 $ 17.50+.50/0 *Chem. Eur. J.* **2002**, *8*, No. 4

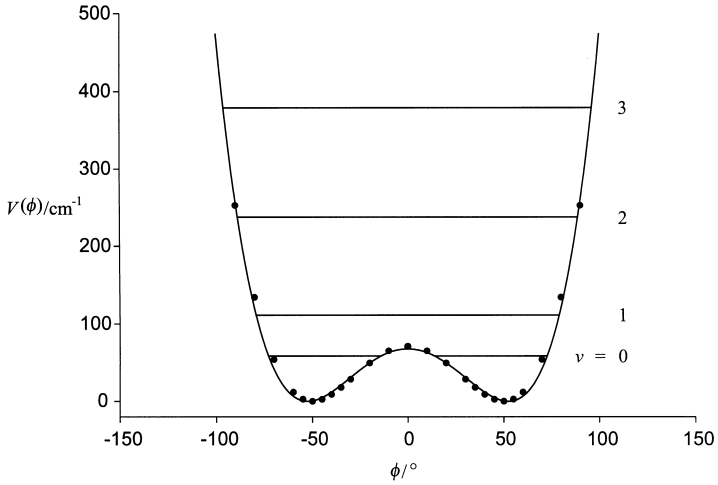

Figure 2. The variation of the potential energy $V(\phi)$ of $H_2O\cdots Br_2$ with the angle ϕ as obtained by ab initio calculations at the aug-cc-pVDZ/MP2 level of theory (see text for discussion). The solid dots are the energies obtained at angles in the range 0° to ±90° from the ab initio calculations. The solid line is the function $V(\phi)=\alpha\phi^4+\beta\phi^2$ obtained by a least-squares fit to the ab initio points. The horizontal lines are vibrational energy levels obtained by solving the one-dimensional oscillator energy eigenvalue problem in the reduced dimensionless coordinate z (see text for details).

Table 6. Experimental and ab initio geometries of H_2O, Br_2 and the complex $H_2O\cdots Br_2$.

Molecule		Geometry	
		ab initio calculation[a]	experiment[b]
Br_2	r(Br–Br)[Å]	2.32383	2.28326[c]
H_2O	r(O–H)[Å]	0.9658	0.9650[d]
	∢ H-O-H [°]	103.670	104.8[d]
$H_2O\cdots Br_2$	r(O – H)[Å]	0.9672	–
	∢ H-O-H [°]	104.99	–
	ϕ [°]	45.75[e]	46.8(1)
	θ [°]	0.8[f]	0.0 (assumed)
	r(O$\cdots$Br)[Å]	2.7908	2.8506(1)

[a] Ab initio geometries are equilibrium quantities. [b] Experimental geometries are r_0-quantities. Values for $H_2O\cdots Br_2$ were determined by fitting values of $I_b + I_c$ for eight isotopomers of the complex. [c] Ref. [20]. [d] Ref. [18]. See Table 5 and footnote [b] for method of determination. [e] ϕ is the angle between the C_2 axis of H_2O and the O$\cdots$Br internuclear axis, as defined in Figure 1. [f] θ is the angular deviation of the nuclei O$\cdots$Br$_i$–Br$_o$ from collinearity.

ab initio calculation at the 6-311 ++ G**/MP2 level of theory due to Alkorta et al.[27] yielded $r_e(O\cdots Br_i)=2.823$ Å, also in good agreement with experiment. No value of ϕ_e is quoted in reference [27].

It is possible to represent the ab initio pairs of points {ϕ, $V(\phi)$} by means of the familiar simple functional form given in Equation (3), which has found much success in describing the observed vibrational spectra associated with ring-puckering and ring-bending modes of four- and five-membered ring molecules.[28]

$$V(\phi)=\alpha\phi^4+\beta\phi^2 \tag{3}$$

It has also been applied to account for the variation of the rotational constants and the electric dipole moment of $H_2O\cdots$HF with the low frequency, out-of-plane intermolecular bending quantum number.[29] A least squares fit of the ab initio points {ϕ, $V(\phi)$} to Equation (3) gave the values $\alpha=$ 97.1(17) cm^{-1} and $\beta=$ -162.4(34) cm^{-1}. This corresponds to a function with $\phi_e=52.4°$ and a potential energy barrier $V(\phi_e)-V(\phi=0)=68.0$ cm^{-1}.

To find values of the vibrational energy levels associated with motion described by the angle ϕ, which corresponds to the low-frequency intermolecular bending mode, it was first necessary to re-express $V(\phi)$ in terms of the familiar one-dimensional reduced coordinate z. The form of $V(z)$ is then[28] that given in Equation (4), where the equations relating α and β to the coefficients a and b are[29] those in Equations (5) and (6).

$$V(z)=a\,(z^4+bz^2) \tag{4}$$

$$a=\alpha^{1/3}\{(r\cos\tfrac{1}{2}\theta)^4\,(2\mu/\hbar^2)^2\}^{-3} \tag{5}$$

$$b=\beta a^{-2}(r\cos\tfrac{1}{2}\theta)^{-2}\,(2\mu/\hbar^2)^{-1} \tag{6}$$

In Equations (5) and (6), r is the distance O–H, θ is the angle H-O-H and μ is the reduced mass for the motion defined by the angle ϕ. The reduced mass can be expressed in terms of the atomic masses and interatomic distances of the complex by means of a simple model of the motion, using an expression given elsewhere[29] for $H_2O\cdots$HF. The values $a=42.15$ cm^{-1} and $b=-2.54$ were obtained in this way. The solution of the energy eigenvalue problem for a one-dimensional oscillator governed by a function defined by Equation (4) and these values of a and b was effected by means of the program ANHARM.[30] The basis set employed consisted of 50 harmonic oscillator functions. The resulting values of E_v for $v=0$,1, 2 and 3, expressed as wavenumbers, are shown drawn to scale in Figure 2. The $v=0$ level lies only 9 cm^{-1} below the top of the potential energy barrier, thereby confirming that, even though it is pyramidal at equilibrium, $H_2O\cdots Br_2$ is effectively planar in the zero-point state according to the definition made in the preceding section.

The quantity $\phi_0\approx\cos^{-1}\langle\cos^2\phi\rangle^{1/2}_{0,0}=46.2(1)°$ was determined by fitting zero-point moments of inertia. Does the one-dimensional potential energy function $V(\phi)$ determined ab initio allow a theoretical prediction of ϕ_0? It is straight forward to obtain a value of $\langle\cos\phi\rangle_{0,0}$ by first expanding it as a Maclaurin series to give Equation (7).

$$\langle\cos\phi\rangle_{0,0}=1-\tfrac{1}{2}\langle\phi^2\rangle_{0,0}+\tfrac{1}{24}\langle\phi^4\rangle_{0,0}-\ldots \tag{7}$$

The transformation expressions (5) and (6) give the required relation $\phi=0.81173\,z$ and the ANHARM program provides values of the averages $\langle z^2\rangle_{0,0}$ and $\langle z^4\rangle_{0,0}$. It is then straight forward to use Equation (7) to obtain $\langle\cos\phi\rangle_{0,0}=$ 0.7790. Under the approximation that $\langle\cos^2\phi\rangle_{0,0}\approx\langle\cos\phi\rangle^2_{0,0}$, we obtain $\phi_0\approx\cos^{-1}\langle\cos\phi\rangle_{0,0}=38.8°$, which is in reasonable agreement with the experimental quantity $\phi_0=46.2(1)°$.

Electron transfer on formation of $H_2O\cdots Br_2$: In view of the definition $\chi_{gg}(Br_x)=eq_{gg}(Br_x)Q(Br_x)$, where $x=$ i (inner) or o (outer), $-q_{gg}(Br_x)$ is the electric field gradient at nucleus x along the principal inertial axis g and $Q(Br_x)$ is the magnitude of the electric quadrupole moment of the nucleus Br_x, it

follows that the experimentally determined principal axis nuclear quadrupole coupling constants $\chi_{gg}(Br_x)$ carry information about the electric charge distribution in Br_2 within $H_2O\cdots Br_2$.

It has been shown elsewhere that the Townes–Dailey model[31, 32] for interpreting nuclear quadrupole coupling constants provides a very simple relation between the values $\chi^e_{zz}(Br_x)$ (x = i or o) of the coupling constants along the Br_2 internuclear axis, z, in the hypothetical equilibrium geometry of complexes such as $H_2O\cdots Br_2$ and the nuclear quadrupole coupling constants $\chi_0(Br_x)$ of free Br_2 and $\chi_A(Br_x)$ of the free Br atom. If a fraction $\delta(O\rightarrow Br_i)$ of an electron is transferred from O to the $4p_z$ orbital of Br_i, while a fraction $\delta(Br_i\rightarrow Br_o)$ is transferred from $4p_z$ of Br_i to $4p_z$ of Br_o, the net increases in population of the respective $4p_z$ orbitals are those shown in Equations (8) and (9), respectively.

$$\delta(Br_i)=\delta(O\rightarrow Br_i)-\delta(Br_i \longrightarrow Br_o) \quad (8)$$

$$\delta(Br_o)=\delta(Br_i \longrightarrow Br_o) \quad (9)$$

Application of the Townes–Dailey model in its simplest form provides the following general Equation (10) relating $\delta(Br_x)$ (x = i or o) to $\chi^e_{zz}(Br_x)$, $\chi_0(Br_x)$ and $\chi_A(Br_x)$.

$$\chi^e_{zz}(Br_x)=\chi_0(Br_x)-\delta(Br_x)\chi_A(Br_x) \quad (10)$$

In good approximation, the equilibrium coupling constant $\chi^e_{zz}(Br_x)$ and the zero-point value $\chi_{aa}(Br_x)$ in $H_2O\cdots Br_2$ are related according to Equation (11).

$$\chi_{aa}(Br_x)=\chi^e_{zz}(Br_x)\langle P_2(\cos\beta)\rangle \quad (11)$$

In Equation (11), β is the instantaneous angle between the a inertia axis and the Br_2 internuclear axis z, P_2 is the second Legendre coefficient and the average is over the zero-point motion of the complex. The use of an exact equality in Equation (11) implies the assumption that the $\delta(Br_x)$ defined in Equations (8) and (9) are independent of the angle ϕ (see Figure 1).

By combining Equations (10) and (11), Equation (12) results.

$$\delta(Br_x)=\{\chi_0(Br_x)/\chi_A(Br_x)\}-\{\chi_{aa}(Br_x)/\chi_A(Br_x)\}\langle P_2(\cos\beta)\rangle^{-1} \quad (12)$$

It is clear that if $\langle P_2(\cos\beta)\rangle$ is known, Equation (12) will give $\delta(Br_i)$ and $\delta(Br_o)$ and thence, from Equations (8) and (9), the fractions $\delta(O\rightarrow Br_i)$ and $\delta(Br_i\rightarrow Br_o)$ of inter- and intramolecular electron transfer on formation of the complex.

An estimate of $\langle P_2(\cos\beta)\rangle$ is available as follows. Ab initio calculations for various complexes $B\cdots Br_2$ have shown[33] that when these complexes are formed from the components the resulting redistribution of charge leads to values of $\chi^e_{zz}(Br_i)$ and $\chi^e_{zz}(Br_o)$ increased and decreased in magnitude relative to $\chi_0(Br)$ of the free Br_2 molecule by almost equal amounts, so that Equation (13) results.

$$\chi^e_{zz}(Br_i)+\chi^e_{zz}(Br_o)\approx 2\chi_0(Br) \quad (13)$$

Combining Equations (11) and (13), we have Equation (14) for $B\cdots {}^{79}Br_2$, for example.

$$\chi_{aa}(Br_i)+\chi_{aa}(Br_o)\approx\chi_0(Br)\langle 3\cos^2\beta-1\rangle \quad (14)$$

It has been shown elsewhere[34] for $OC\cdots {}^{79}Br_2$ that application of Equation (14) leads to $\beta_{av}=\cos^{-1}\langle\cos^2\beta\rangle^{1/2}=6.12^\circ$. The result for $H_2O\cdots {}^{79}Br_2$ obtained by using the appropriate nuclear quadrupole coupling constants from Table 3 and $\chi_0({}^{79}Br)$ from Table 5 gives $\beta_{av}=5.81^\circ$. The smaller value for the H_2O complex than $OC\cdots {}^{79}Br_2$ is consistent with the weaker binding (as indicated by the smaller value of the intermolecular stretching force constant k_σ) in the latter case and therefore smaller angular oscillations of the Br_2 subunit. We shall use the value $\beta_{av}=5.5(5)^\circ$ in $H_2O\cdots Br_2$ with some confidence that the true value lies some where in the range $\pm 0.5^\circ$.

Values of $\delta(O\cdots Br_i)$ and $\delta(Br_i\rightarrow Br_o)$ determined by use of Equation (12), (8) and (9) together with appropriate values of the nuclear quadrupole coupling constants $\chi_{aa}(Br_x)$, $\chi_0(Br_x)$[35] and $\chi_A(Br_x)$[36] from Tables 3–5 are recorded in Table 7. The errors in the fractions of electron transferred are those propagated from the assumed range in β_{av} and are fortunately small. We note from Table 7 that the fraction of an electron $\delta(O\cdots Br_i)$ transferred from H_2O to Br_i is almost negligibly small while the fraction simultaneously transferred from Br_i to Br_o (i.e., a polarisation of Br_2) is considerably larger. Thus, the net change in electron population at Br_i is predominantly the result of intramolecular redistribution within Br_2.

Table 7. Values of $\delta(O\rightarrow Br_i)$ and $\delta(Br_i\rightarrow Br_i)$ determined from Br nuclear quadrupole coupling constants[a] and k_σ determined from the centrifugal distortion constant Δ_J.[b]

Isotopomer	$\delta(O\rightarrow Br_i)$	$\delta(Br_i\rightarrow Br_i)$	k_σ [N m^{-1}]
$H_2O\cdots {}^{79}Br{}^{79}Br$	0.004(5)	0.050(2)	9.9(1)
$H_2O\cdots {}^{81}Br{}^{79}Br$	0.004(5)	0.050(2)	10.1(1)
$H_2O\cdots {}^{79}Br{}^{81}Br$	0.003(5)	0.049(2)	9.7(1)
$H_2O\cdots {}^{81}Br{}^{81}Br$	0.003(5)	0.049(2)	9.8(1)
$D_2O\cdots {}^{79}Br{}^{81}Br$	0.005(5)	0.050(2)	9.6(1)
$D_2O\cdots {}^{81}Br{}^{81}Br$	0.004(5)	0.050(2)	9.6(1)
$HDO\cdots {}^{79}Br{}^{81}Br$	0.004(5)	0.050(2)	9.2(2)
$HDO\cdots {}^{81}Br{}^{81}Br$	0.004(5)	0.050(2)	10.7(3)

[a] $\delta(O\rightarrow Br_i)$ and $\delta(Br_i\rightarrow Br_i)$ are the fractions of an electronic charge transferred from O to Br_i and from Br_i to Br_o, respectively, on complex formation, as determined by the method discussed in the text. [b] k_σ determined by use of Δ_J in Equation (15).

Intermolecular stretching force constant k_σ: The strength of the intermolecular binding in $H_2O\cdots Br_2$ may be gauged from the magnitude of the quadratic intermolecular stretching force constant k_σ. This quantity is proportional to the energy required for a unit infinitesimal displacement along the $O\cdots Br_i$ direction. Millen[37] showed that, in the approximation of rigid subunits B and XY and when contributions from cubic and higher force constants are ignored, k_σ is related to the centrifugal distortion constant Δ_J for a planar asymmetric rotor complex $B\cdots XY$ of C_{2V} symmetry through Equation (15).

$$k_\sigma=(8\pi^2\mu_c/\Delta_J)\{B^3(1-b)+C^3(1-c)-\tfrac{1}{4}(B-C)^2(B+C)(2-b-c)\} \quad (15)$$

0947-6539/02/0804-0948 $ 17.50+.50/0 Chem. Eur. J. 2002, 8, No. 4

In Equation (15), B and C are rotational constants of the complex, $\mu_c = m^B m^{XY}/(m^B + m^{XY})$ is the reduced mass associated with stretching of the intermolecular bond, $b = (B/B_B) + (B/B_{XY})$ and c is the corresponding quantity defined in terms of the rotational constants C, C_B and C_{XY} of the complex, the Lewis base B and the dihalogen molecule XY, respectively. Although $H_2O\cdots XY$ has a pyramidal *equilibrium* configuration at O, in the zero-point state the complex is effectively planar (see preceding sections) and, of the available expressions, that given by Equation (15) is the most appropriate.

Values of k_σ calculated from the Δ_J, B_0, C_0 values of the complex (Tables 3 and 4) and the appropriate zero-point rotational constants of H_2O[18, 19] and Br_2[20] (given in Table 5) are shown in Table 7 for each of the isotopomers investigated. The errors quoted are those propagated from the experimental errors in Δ_J, which are predominant. Systematic errors in the model are presumably responsible for an isotopic variation in k_σ that exceeds the range implied by the experimental errors.

Discussion

The ground-state rotational spectra of eight isotopomers of the complex $H_2O\cdots Br_2$ have been recorded by using a pulsed-jet, Fourier-transform microwave spectrometer in conjunction with a fast-mixing nozzle. Spectroscopic constants determined by fitting assigned spectra have been interpreted with the aid of models of the complex to yield a number of its properties. Thus, it has been established that $H_2O\cdots Br_2$ has a geometry of C_s symmetry at equilibrium with a pyramidal arrangement of the two H atoms and the atom Br_i around the oxygen atom. Ab initio calculations conducted at the aug-cc-pVDZ/MP2 level of theory give predictions for the distance $r(O\cdots Br_i)$ and the angle ϕ (as defined in Figure 1) that are in reasonable agreement with the zero-point values of these quantities obtained by fitting experimental ground-state moments of inertia. The intermolecular charge transfer on formation of $H_2O\cdots Br_2$ is almost negligible. This is indicated by the quantity $\delta(O\rightarrow Br_i) = 0.004(5)$, which is the fraction of an electron transferred from O to Br_i, as estimated from the Br nuclear quadrupole coupling constants using an interpretation based on the Townes–Dailey model for relating electric field gradients and electronic structure. The interaction of H_2O and Br_2 in the complex is weak, as shown by the value $k_\sigma = 9.8(2)\ Nm^{-1}$ of the intermolecular stretching force constant determined from the centrifugal distortion constant. The resistance to inversion of the configuration is also small in view of the fact that, according to the ab initio calculations, the zero-point energy level lies only a few cm^{-1} below the top of the potential energy barrier at the planar C_{2V} form of the complex.

A similar approach to that described in the preceding paragraph has now been applied to six complexes of the type $H_2O\cdots XY$, namely those in which XY is F_2,[6, 7] Cl_2,[9] Br_2, BrCl,[10] ClF[7, 8] and ICl.[11] It is timely to compare the properties of the complexes determined in this way. Collected in Table 8 are the experimental zero-point quantities $r(O\cdots X)$ and ϕ_0, the equilibrium angle ϕ_e and the potential energy barrier $\{V(\phi_e) - V(\phi = 0)\}$ from ab initio calculations, the fractions $\delta(O\rightarrow X)$ and $\delta(X\rightarrow Y)$ of an electron transferred inter- and intramolecularly on complex formation, and the intermolecular stretching force constants k_σ. The values of $\{V(\phi_e) - V(\phi = 0)\}$ and ϕ_e for $H_2O\cdots ICl$ are not strictly comparable with those for the other members of the series because a different type of basis function was used in its ab initio calculation[11] and because the geometry was not optimised at each angle ϕ, but instead the experimental H_2O and ICl geometries were assumed and were taken to be independent of ϕ.

Several conclusions of interest may be drawn from the comparisons in Table 8. Firstly, the strength of the interaction, as defined by k_σ, increases in the order $F_2 < Cl_2 < Br_2 <$ BrCl < ClF < ICl. In the case of the nonpolar dihalogens, this is the order of their electric quadrupole moments which have the values 2.8×10^{-40}, $10.8(5)\times10^{-40}$ and $17.5\times10^{-40}\ Cm^2$ for F_2, Cl_2 and Br_2, respectively.[38, 39] The complexes in which the dihalogen is polar are all more strongly bound than those involving nonpolar species and the order is the order of the electric dipole moments of the halogen, namely BrCl[40] < ClF[41] < ICl.[42]

Secondly, with the exception of $H_2O\cdots ICl$, the order of the potential energy barrier $V(\phi_e) - V(\phi = 0)$ follows the order of the binding strength. It seems likely that a more sophisticated ab initio calculation for $H_2O\cdots ICl$ will lead to a result in excess of 174 cm^{-1}, therefore.

Thirdly, the extent of intermolecular electron transfer $\delta(O\rightarrow X)$ is almost negligible across the series, rising to only one hundredth of an electron in $H_2O\cdots ICl$. Such a small electron transfer is consistent with a high ionization energy $I_{H_2O} = 12.61(6)$ eV of the H_2O molecule.[43] On the other hand, the intramolecular electron transfer is more significant and

Table 8. Comparison of some properties of complexes $H_2O\cdots XY$, where $XY = F_2$, Cl_2, Br_2, BrCl, ClF and ICl, as determined by rotational spectroscopy and ab initio calculations.

Property	Complex					
	$H_2O\cdots F_2$[a]	$H_2O\cdots Cl_2$[b]	$H_2O\cdots Br_2$[c]	$H_2O\cdots BrCl$[d]	$H_2O\cdots ClF$[a]	$H_2O\cdots ICl$[e]
$r(O\cdots X)$[Å][f]	2.748(3)	2.8479(3)	2.8506(1)	2.7809(3)	2.608(2)	2.6109(6)
ϕ_0 [°][f]	48.5(20)	43.4(3)	46.8(1)	47.9(2)	58.9(2)	60.8(4)
ϕ_e [°][g]	41.7	47.7	45.7	54.6	55.8	≈45°
$\{V(\phi_e) - V(\phi = 0)\}$[$cm^{-1}$][g]	7	42	68	99	174	≈100
$\delta(O\rightarrow X)$[h]	···	0.005(5)	0.005(5)	0.009(5)	···	0.010(4)
$\delta(X\rightarrow Y)$[h]	···	0.034(3)	0.050(2)	0.053(3)	···	0.065(1)
k_σ [$N m^{-1}$][i]	3.7(1)	8.0(1)	9.8(2)	12.1(1)	14.2(1)	15.7(3)

[a] Ref. [7]. [b] Ref. [9]. [c] This work. [d] Ref. [10]. [e] Ref. [11]. [f] Zero-point quantities estimated by fitting $I_b^0 + I_c^0$ as described here and in appropriate references. [g] Equilibrium values of ϕ and the barrier height in the potential energy function determined by ab initio methods described in the text. For $H_2O\cdots ICl$ a different type of basis set was used and the experimental geometry was used at each point. Hence these values should be treated with caution. [h] Fractions of electron transferred from O to X or X to Y (see text for definition). These quantities are not available for $H_2O\cdots F_2$ and $H_2O\cdots ClF$. [i] As determined using Δ_J in Equation (15).

appears to increase as the polarizability of the front end atom increases, with order $Cl_2 < Br_2 \sim BrCl < ICl$.

Finally, we note the result that all complexes, even $H_2O \cdots F_2$,[7] have a pyramidal configuration at O and C_s symmetry at the equilibrium geometry. This makes it clear that all of these complexes obey the rule originally put forward to account for the observed geometries of hydrogen-bonded complexes $B \cdots HX$[44, 45] and recently extended[4, 5] to include complexes $B \cdots XY$ involving dihalogen molecules. The rules require that the nucleophilic end $^{\delta+}H$ of HX or $^{\delta+}X$ of XY seeks the axis of a nonbonding or π-bonding electron pair carried by the electron-donor atom of B. In the case of H_2O, the angle between the nonbonding electron pairs is $\approx 109^\circ$, so that ϕ_e should be $\approx 50^\circ$ in these complexes, as indeed it is. Similar conclusions have been reached for $H_2O \cdots HF$[29] and $H_2O \cdots HCl$,[21] strengthening the case for the halogen bond in $B \cdots XY$ complexes, as recently postulated.[4, 5]

Experimental Section

The ground-state rotational spectra of eight isotopomers of $H_2O \cdots Br_2$ were observed with a pulsed-jet, Fourier-transform microwave spectrometer. The design of the instrument was based on the prototype described by Balle and Flygare[46] but with two sets of modifications, as discussed elsewhere.[14, 10] To avoid any possibility of a reaction between H_2O and Br_2 a fast-mixing nozzle[13] was employed in the spectrometer as the source of complexes. The vapour from above a room-temperature sample of water was flowed continuously through the central, 0.3 mm internal diameter glass capillary of this device into the evacuated Fabry–Pérot cavity of the spectrometer. A gas mixture composed of 2% bromine (Aldrich) and 98% argon was pulsed, from a stagnation vessel held at a total pressure of 3 bar, down the outer tube of the nozzle at a rate of 3–5 Hz. The pulses were of about 1 ms in length and were produced by a Series 9 solenoid valve (Parker Hannifin). Complexes formed at the cylindrical interface of the two gas flows as they expanded from the concentric inner and outer tubes of the mixing nozzle into the Fabry–Pérot cavity perpendicular to its axis were rotationally polarised by 1 μs pulses of microwave radiation. The subsequent free induction decay at rotational transition frequencies of the complexes was detected and processed in the usual manner. The full width at half height of individual Br nuclear quadrupole hyperfine components in the spectrum of $H_2O \cdots Br_2$ observed in this way was about 20 kHz and led to an accuracy of frequency measurement estimated to be 2 kHz.

Rotational spectra of $D_2O \cdots Br_2$ and $HDO \cdots Br_2$ isotopomers were observed by flowing either D_2O (Appollo Scientific Ltd., 99.8% D) or an equimolar mixture of D_2O and H_2O, respectively, through the mixing nozzle.

Acknowledgement

We thank the Engineering and Physical Sciences Research Council for a studentship (J.M.A.T.) and a Senior Fellowship (A.C.L.). We also thank the Leverhulme Trust for a research grant in support of the work described here and J.M.A.T. thanks the Society of Chemical Industry for the award of a Messel Scholarship. We are grateful to James Davey for help with the ab initio calculations.

[1] *Gmelin Handbook of Inorganic Chemistry*, Br, *Supplement Vol. A*, Element, Eighth Edition, Springer, Berlin, **1985**, pp. 429–446.
[2] J. P. D. Abbatt, *Geophys. Res. Lett.* **1994**, *21*, 665–668.
[3] L. Chu, L. T. Chu, *J. Phys. Chem.* **1999**, *103*, 691–699.
[4] A. C. Legon, *Chem. Eur. J.* **1998**, *4*, 1890–1897.
[5] A. C. Legon, *Angew. Chem.* **1999**, *111*, 2850–2880; *Angew. Chem. Int. Ed.* **1999**, *38*, 2686–2714.
[6] S. A. Cooke, G. Cotti, J. H. Holloway, A. C. Legon, *Angew. Chem.* **1997**, *109*, 81–83; *Angew. Chem. Int. Ed. Engl.* **1997**, *36*, 129–130.
[7] S. A. Cooke, G. Cotti, C. M. Evans, J. H. Holloway, Z. Kisiel, A. C. Legon, J. M. A. Thumwood, *Chem. Eur. J.* **2001**, 7, 2295–2305.
[8] S. A. Cooke, G. Cotti, C. M. Evans, J. H. Holloway, A. C. Legon, *Chem. Commun.* **1996**, 2327–2328.
[9] J. B. Davey, A. C. Legon, J. M. A. Thumwood, *J. Chem. Phys.* **2001**, *114*, 6190–6202.
[10] J. B. Davey, A. C. Legon, *Phys. Chem. Chem. Phys.* **2001**, *3*, 3006–3011.
[11] J. B. Davey, A. C. Legon, E. R. Waclawik, *Phys. Chem. Chem. Phys.* **2000**, *2*, 1659–1665.
[12] A. Engdahl, B. Nelander, *J. Chem. Phys.* **1986**, *84*, 1981–1987.
[13] A. C. Legon, C. A. Rego, *J. Chem. Soc. Faraday Trans.* **1990**, *86*, 1915–1921.
[14] A. C. Legon in *Atomic and Molecular Beam Methods*, *Vol. 2*, (Ed. G. Scoles), Oxford University Press, Oxford **1992**, Chapter 9, pp. 289–308.
[15] H. M. Pickett, *J. Mol. Spectrosc.* **1991**, *148*, 371–377.
[16] J. K. G. Watson, *J. Chem. Phys.* **1968**, *48*, 4517–4524.
[17] A. C. Legon, *Faraday Discuss. Chem. Soc.* **1988**, *86*, 269–270.
[18] R. L. Cook, F. C. DeLucia, P. Helminger, *J. Mol. Spectrosc.* **1974**, *53*, 62–76.
[19] J. Bellet, W. J. Lafferty, G. Steenbeckeliers, *J. Mol. Spectrosc.* **1973**, *47*, 388–402.
[20] R. F. Barrow, T. C. Clark, J. A. Coxon, K. K. Lee, *J. Mol. Spectrosc.* **1974**, *51*, 428–438.
[21] Z. Kisiel, B. A. Pietrewicz, P. W. Fowler, A. C. Legon, E. Steiner, *J. Phys. Chem. A.* **2000**, *104*, 6970–6978.
[22] M. W. Schmidt, K. K. Baldridge, J. A. Boatz, S. T. Elbert, M. S. Gordon, J. H. Jensen, S. Koseki, N. Matsunaga, K. Nguyen, S. J. Su, T. L. Windus, M. Dupuis, J. A. Montgomery, *J. Computat. Chem.* **1993**, *14*, 1347–1363.
[23] T. H. Dunning, Jr. *J. Chem. Phys.* **1989**, *90*, 1007–1023.
[24] R. A. Kendall, T. H. Dunning, Jr., R. J. Harrison, *J. Chem. Phys.* **1992**, *96*, 6796–6806.
[25] C. Mϕller, M. S. Plesset, *Phys. Rev.* **1934**, *46*, 618–622.
[26] S. F. Boys, F. Bernardi, *Mol. Phys.* **1970**, *19*, 553–566.
[27] I. Alkorta, I. Rozas, J. Elguero, *J. Phys. Chem. A.* **1998**, *102*, 9278–9285.
[28] J. Laane, *Appl. Spectrosc.* **1970**, *24*, 73–80.
[29] Z. Kisiel, A. C. Legon, D. J. Millen, *Proc. R. Soc. London A* **1982**, *381*, 419–442.
[30] J. Mjöberg, Program ANHARM, University College London, **1975**.
[31] C. H. Townes, B. P. Dailey, *J. Chem. Phys.* **1949**, *17*, 782–796.
[32] C. H. Townes, A. L. Schawlow, *Microwave Spectroscopy*, McGraw Hill, New York, **1955**, Chapter 9, pp. 225–247.
[33] P. W. Fowler, S. A. Peebles, A. C. Legon, *Adv. Quantum Chem.* **1997**, *28*, 248–255.
[34] E. R. Waclawik, J. M. A. Thumwood, D. G. Lister, P. W. Fowler, A. C. Legon, *Mol. Phys.* **1999**, *97*, 159–166.
[35] N. Bettin, H. Knöckel, E. Tiemann, *Chem. Phys. Lett.* **1981**, *80*, 386–388.
[36] W. Gordy, R. L. Cook, *Microwave Molecular Spectra*, *vol XVIII*, in *Techniques of Chemistry*, (Ed.: A. Weissberger) Wiley-Interscience, New York, **1984**, Chapter 14.
[37] D. J. Millen, *Can. J. Chem.* **1985**, *63*, 1477–1479.
[38] S. A. Peebles, P. W. Fowler, A. C. Legon, unpublished results.
[39] A. D. Buckingham, C. Graham, J. H. Williams, *Mol. Phys.* **1983**, *49*, 703–710.
[40] K. P. R. Nair, J. Hoeft, E. Tiemann, *Chem. Phys. Lett.* **1978**, *58*, 153–156.
[41] B. Fabricant, J. S. Muenter, *J. Chem. Phys.* **1977**, *66*, 5274–5277.
[42] E. Herbst, W. Steinmetz, *J. Chem. Phys.* **1972**, *56*, 5342–5353.
[43] D. W. Turner, C. Baker, A. D. Baker, C. R. Brundle, *Molecular Photoelectron Spectroscopy*, Wiley-Interscience, London, **1970**, Chapter 4, pp. 61–131.
[44] A. C. Legon, D. J. Millen, *Faraday Discuss. Chem. Soc.* **1982**, *73*, 71–87.
[45] A. C. Legon, D. J. Millen, *Chem. Soc. Rev.* **1987**, *16*, 467–498.
[46] T. J. Balle, W. H. Flygare, *Rev. Sci. Instrum.*, **1981**, *52*, 33–45.

Received: June 11, 2001 [F3323]

  0947-6539/02/0804-0950 $ 17.50+.50/0